Effect of Baroclinicity on Wind Profiles and the Geostrophic Drag Law for the Convective Planetary Boundary Layer[1]

S. P. S. ARYA AND J. C. WYNGAARD[2]

Department of Atmospheric Sciences, University of Washington, Seattle 98195

(Manuscript received 20 August 1974, in revised form 3 December 1974)

ABSTRACT

By using a simple physical model of the baroclinic convective planetary boundary layer, the similarity functions of the geostrophic drag law are expressed as sums of a barotropic part, dependent only on the stability and boundary layer height parameters, and a baroclinicity dependent part. The latter are predicted to be sinusoidal functions of the angle between surface wind and geostrophic shear, their amplitudes being proportional to the normalized magnitude of geostrophic shear. These drag laws are confirmed by the results of a more sophisticated higher-order closure model, which also predict the magnitude of actual wind shears in the bulk of the mixed layer remaining much smaller than the magnitude of imposed geostrophic shear. The results are shown to be supported by some observations from the recent Wangara and ATEX experiments. The surface cross-isobar angle is predicted to increase toward the equator, a trend well confirmed by observations, but in obvious conflict with the drag laws proposed by others who have ignored the height of the lowest inversion base from their similarity considerations.

1. Introduction

Empirical determinations of the stability-dependent similarity functions of geostrophic drag laws usually result in a large scatter of data points (Zilitinkevich and Chalikov, 1968; Arya, 1975; Clarke and Hess, 1974; Melgarejo and Deardorff, 1974). Some of it, of course, is due to uncertainties in the measurements of geostrophic winds and surface fluxes. We suggest a large part of the scatter, however, is due to the effects of baroclinicity and accelerations. We wish to investigate here the effects of baroclinicity, using a simple physical model of the convective planetary boundary layer. The results will be verified by a more sophisticated higher-order closure model developed by Wyngaard *et al.* (1974), and will be compared with observations in the atmosphere.

The geostrophic shear or baroclinicity is related to temperature gradients through the well known "thermal wind" equations

$$\left.\begin{aligned}\frac{\partial U_g}{\partial z}&=-\frac{g}{fT}\frac{\partial T}{\partial y}+\frac{U_g}{T}\frac{\partial T}{\partial z}\\ \frac{\partial V_g}{\partial z}&=\frac{g}{fT}\frac{\partial T}{\partial x}+\frac{V_g}{T}\frac{\partial T}{\partial z}\end{aligned}\right\}. \tag{1}$$

The terms "thermal wind," "geostrophic shear" and "baroclinicity" are used interchangeably; they are all considered equivalent. We use a right-hand coordinate system with x and y axes in the horizontal plane and the z axis in the vertical; T denotes the absolute temperature, f the Coriolis parameter; and $U_g=-(1/f\rho)(\partial p/\partial y)$ and $V_g=(1/f\rho)(\partial p/\partial x)$ are the geostrophic wind components (p and ρ being air pressure and density).

The second terms on the right-hand side of (1) are usually ignored; their contribution to the geostrophic shear is, at most, 4% per kilometer under neutral and unstable conditions when the lapse rate in the bulk of the planetary boundary layer is close to the dry adiabatic lapse rate of about 0.01°C m^{-1}. Large geostrophic shears arise from large horizontal temperature gradients, typical of the mesoscale systems such as fronts, sea breezes, slope and valley winds, etc. But even in an idealized planetary boundary layer above a homogeneous and featureless terrain, some baroclinicity is to be expected due to the climatological north-south temperature gradient. For example, a gradient of 1°C (100 km)$^{-1}$, which is not uncommon, gives rise to a geostrophic shear of as large as 3.5 m s^{-1} km^{-1}, in middle latitudes. Thus baroclinicity in the lower atmosphere is a rule rather than the exception, but its effects on the structure and parametric relations of the boundary layer remain poorly understood.

2. Previous studies

Sheppard *et al.* (1952) and Sheppard and Omar (1952) were probably the first to demonstrate through their observations over the sea (near-neutral stability) the

[1] Contribution No. 324, Department of Atmospheric Sciences, University of Washington.

[2] Air Force Cambridge Research Laboratories, Bedford, Mass. 01730.

large effects of baroclinicity on the wind shear as well as on the surface cross-isobaric angle α_0. More detailed empirical determinations of thermal wind effects on α_0 and the ratio V_0/G_0 of the surface wind (at some reference level) to the surface geostrophic wind, which is indirectly related to the drag coefficient, have been made by Bernstein (1959) and Hoxit (1974). In both cases, a large number of routine radiosonde and rawinsonde data from a number of stations in the eastern half of the United States have been analyzed. The scatter in α_0 for individual observations is extremely large and, in order to see any trend with thermal winds, many data had to be averaged regardless of location (surface roughness) and time (thermal stability). Although there is a fair amount of subjectivity involved in the interpretation of these averaged data, they do indicate that α_0 increases considerably during warm air advection and decreases during cold air advection. The ratio V_0/G_0 is observed to increase when geostrophic shear is oriented with surface wind and to decrease when it is in the opposite direction. Considerable observational evidence on the effect of thermal winds on the actual wind veering in the planetary boundary layer has been reported by Lettau (1967) and Gray and Mendenhall (1973).

Theoretical explanations of the above observations have been sought primarily through the use of K-theory models in which assumptions are made about eddy viscosity or mixing length distributions in the boundary layer with a constant or exponentially decreasing thermal wind (Ellison, 1956; Lettau, 1967; Bernstein, 1959; Mahrt and Schwerdtfeger, 1970; Wippermann, 1972; Venkatesh and Csanady, 1974). A serious limitation of such models is that possible modifications of eddy viscosity or mixing length by geostrophic shear (see Vorob'yev, 1969) are not taken into account. Moreover, in convective conditions, the very concept of eddy viscosity or eddy diffusivity becomes meaningless, because considerable heat and momentum transfer occur primarily through the aid of buoyancy, while the mean gradients are close to zero or even of "wrong" sign (see Deardorff, 1966, 1972; Wyngaard *et al.*, 1974a, b).

3. A simple model for drag laws in the baroclinic case

Previously (Wyngaard *et al.*, 1974a) we suggested a mechanism by which convective activity limits the mean wind shear in the planetary boundary layer. For the steady-state barotropic case, we argued that the conservation equations for stress and mean shear form a feedback system which drives the wind shear to minimal levels in the mixed layer. We showed that buoyancy activates the feedback system through the vertical velocity variance.

We suggest that this control mechanism also limits wind shear magnitudes in the baroclinic case. Taking steady-state convective conditions, we start with the mean shear equations

$$\left.\begin{aligned}\frac{\partial^2\overline{uw}}{\partial z^2}&=f\left(\frac{\partial V}{\partial z}-\frac{\partial V_g}{\partial z}\right)\\ \frac{\partial^2\overline{vw}}{\partial z^2}&=f\left(\frac{\partial U_g}{\partial z}-\frac{\partial U}{\partial z}\right)\end{aligned}\right\}, \tag{2}$$

where u, v, w denote the fluctuating velocity components and U, V, W (~ 0) the mean flow components in the x, y, z directions, respectively. We assume that the mean wind shear magnitude is not small, but is comparable to the magnitude of geostrophic shear. Then, according to Eq. (2), one or both of the stress profile curvatures must remain near zero as in the barotropic case. Large magnitudes of $\partial U/\partial z$ and $\partial V/\partial z$, however, will interact with $\overline{w^2}$ (which becomes quite large under convective conditions) through the conservation equations to produce large magnitudes of $\partial^2\overline{uw}/\partial z^2$ and $\partial^2\overline{vw}/\partial z^2$, in contradiction to Eq. (2). Therefore our original assumption is incorrect and the magnitude of actual wind shear has to remain much smaller than the magnitude of geostrophic shear. One can therefore write for convective conditions

$$\left.\begin{aligned}\frac{\partial^2\overline{uw}}{\partial z^2}&\approx -f\frac{\partial V_g}{\partial z}, \quad \text{when} \quad \frac{\partial V_g}{\partial z}\neq 0\\ \frac{\partial^2\overline{vw}}{\partial z^2}&\approx f\frac{\partial U_g}{\partial z}, \quad \text{when} \quad \frac{\partial U_g}{\partial z}\neq 0\end{aligned}\right\}, \tag{3}$$

provided the atmosphere is not too close to barotropic.

Note that a positive $\partial V_g/\partial z$ requires a negative $\partial^2\overline{uw}/\partial z^2$ and therefore a positive going tendency in the $\overline{uw}$-profile aloft, presumably given by the production term $-\overline{w^2}(\partial U/\partial z)$. This requires a negative $\partial U/\partial z$. Thus the sign of $\partial U/\partial z$ is expected to be opposite to that of $\partial V_g/\partial z$. Similarly, one can trace another loop to show that $\partial V/\partial z$ should have the same sign as $\partial U_g/\partial z$. This, of course, is for the Northern Hemisphere; south of the equator $\partial U/\partial z$ and $\partial V_g/\partial z$ should have the same sign, while those of $\partial V/\partial z$ and $\partial U_g/\partial z$ are opposite. Actual magnitudes of wind shears will also depend on the intensity of convection as measured by z_i/L, where z_i is the height of inversion base and L is Obukhov's length. For large $-z_i/L$, mixing will be quite effective in making $|\partial U/\partial z|$ and $|\partial V/\partial z|$ quite small. More quantitative substantiation of this will be provided later on, using a more sophisticated numerical model as well as some observations of unstable atmospheric boundary layers.

The relatively small wind shears predicted for the steady-state baroclinic convective boundary layer have some interesting consequences for mean flow similarity and the geostrophic drag law. Consider the geostrophic departure equations, which can be written in the form

$$\left.\begin{aligned}\frac{\langle U_g\rangle}{u_*}&=\frac{\langle U\rangle}{u_*}\\ \frac{\langle V_g\rangle}{u_*}&=\frac{\langle V\rangle}{u_*}-\frac{u_*}{fH}\end{aligned}\right\}. \tag{4}$$

Here, the angle brackets denote the average over the boundary layer, and H is the height where stress vanishes and the flow becomes geostrophic. We will roughly estimate H as z_i, although it may actually be somewhat larger (Deardorff, 1974).

In the barotropic case, $U\approx$ constant and $V\approx 0$ in the mixed layer, so that Eqs. (4) reduce to (see also Wyngaard *et al.*, 1974a)

$$\left.\begin{aligned}\frac{U_g}{u_*}&\approx\frac{U}{u_*}\\ \frac{V_g}{u_*}&\approx-\frac{u_*}{fz_i}\end{aligned}\right\}. \tag{5}$$

The universal drag relations for a barotropic convective boundary layer are usually written in the form (Arya, 1975; Melgarejo and Deardorff, 1974)

$$\left.\begin{aligned}A_i&=\ln\frac{z_i}{z_0}-k\frac{U_g}{u_*}\\ B_i&=-k\frac{V_g}{u_*}\operatorname{sign}f\end{aligned}\right\}, \tag{6}$$

in which z_0 is the surface roughness scale and A_i and B_i are presumably some universal similarity functions of z_i/L and fz_i/u_*.

Since we expect wind shear magnitudes in the mixed layer to remain small even in the presence of the typical geostrophic shears in a boundary layer over an homogeneous terrain, one expects that $\langle U\rangle/u_*$ and $\langle V\rangle/u_*$ would roughly correspond to their respective barotropic values for the same z_i/L, z_i/z_0 and fz_i/u_*. Then, a comparison of (4) and (5) suggests that $\langle U_g\rangle/u_*$ and $\langle V_g\rangle/u_*$ should remain more or less independent of geostrophic shear, so that we can generalize (6) by writing

$$\left.\begin{aligned}A_i&=\ln\frac{z_i}{z_0}-k\frac{\langle U_g\rangle}{u_*}\\ B_i&=-k\frac{\langle V_g\rangle}{u_*}\operatorname{sign}f\end{aligned}\right\}. \tag{7}$$

Therefore, the same universal functions A_i and B_i should describe both barotropic and baroclinic cases if layer-averaged geostrophic winds are used. If surface geostrophic winds are used, which might be more convenient in practice, we will denote the functions by A_{i0} and B_{i0}. Note that they will differ from A_i and B_i due to baroclinicity:

$$\left.\begin{aligned}A_{i0}&=\ln\frac{z_i}{z_0}-k\frac{U_{g0}}{u_*}=\ln\frac{z_i}{z_0}-k\frac{\langle U_g\rangle}{u_*}\\ &\qquad -k\left[\frac{U_{g0}-\langle U_g\rangle}{u_*}\right]=A_i+A_i'\\ B_{i0}&=-k\frac{V_{g0}}{u_*}\operatorname{sign}f=-k\frac{\langle V_g\rangle}{u_*}\operatorname{sign}f\\ &\qquad -k\left[\frac{V_{g0}-\langle V_g\rangle}{u_*}\right]=B_i+B_i'\end{aligned}\right\}. \tag{8}$$

Using Eqs. (5), we estimate the universal functions as

$$\left.\begin{aligned}A_i&=\ln\frac{z_i}{z_0}-k\frac{U}{u_*}\\ B_i&=k\frac{u_*}{fz_i}\operatorname{sign}f\end{aligned}\right\}. \tag{9}$$

The representative value of U/u_* for the mixed layer was obtained in our previous study (Wyngaard *et al.*, 1974a) by simply integrating the dimensionless wind shear function from the surface to the top of the surface layer (taken as some fraction of z_i). This gave $A_i\approx\ln(-z_i/L)$, a result surprisingly close to what we obtained (see Table 1) from the higher-order closure model of Wyngaard *et al.* (1974b) and also in fair agreement with the Wangara data. While A_i shows only a very weak dependence on the parameter fz_i/u_*, according to the model results, B_i is inversely proportional to it, as also indicated in the second of Eqs. (9).

The deviations A_i' and B_i' due to thermal winds can easily be expressed as functions of baroclinicity parameters. Following similarity arguments, Hess (1973) and Yordanov and Wippermann (1972) have suggested

TABLE 1. The computed similarity functions for the barotropic unstable boundary layer.

$-\frac{z_i}{L}$	$\frac{fz_i}{u_*}$	A_i	B_i
10	1.0	3.39	0.60
20	1.0	4.34	0.44
50	1.0	5.32	0.37
100	1.0	5.99	0.35
1000	1.0	7.63	0.35
50	0.133	4.05	2.63

the use of

$$\left.\begin{aligned} S_x &= -\frac{1}{f}\frac{\partial U_g}{\partial z} \\ S_y &= -\frac{1}{f}\frac{\partial V_g}{\partial z} \end{aligned}\right\}, \tag{10}$$

which are unique parameters only in the special case of geostrophic shear being invariant with height. In general, S_x and S_y may be taken as

$$\left.\begin{aligned} S_x &= S_{x0}F(\xi_i) \\ S_y &= S_{y0}G(\xi_i) \end{aligned}\right\}, \tag{11}$$

where S_{x0} and S_{y0} are their values at the surface, and F and G are functions of the dimensionless height $\xi_i = z/z_i$. A_i' and B_i' are expected to depend on S_{x0}, S_{y0} and some integral properties of the functions F and G.

The geostrophic wind profiles are given by the integration of Eqs. (11), i.e., by

$$\left.\begin{aligned} \frac{U_g}{u_*} &= \frac{U_{g0}}{u_*} + \frac{fz_i}{u_*}S_{x0}\int_0^{\xi_i} F(\xi_i')d\xi_i' \\ \frac{V_g}{u_*} &= \frac{V_{g0}}{u_*} + \frac{fz_i}{u_*}S_{y0}\int_0^{\xi_i} G(\xi_i')d\xi_i' \end{aligned}\right\}. \tag{12}$$

The layer-averaged values $\langle U_g\rangle/u_*$ and $\langle V_g\rangle u_*$ are obtained by integrating (12) again with respect to ξ_i and taking the limits from $\xi_i=0$ to 1. Then, according to (8),

$$\left.\begin{aligned} A_i' &= a\frac{fz_i}{u_*}S_{x0} \equiv aM_{x0} \equiv aM_0\cos\beta_0 \\ B_i' &= b\frac{fz_i}{u_*}S_{y0} \equiv bM_{y0} \equiv bM_0\sin\beta_0 \end{aligned}\right\}, \tag{13}$$

where the coefficients a and b are given by

$$\left.\begin{aligned} a &= k\int_0^1\int_0^{\xi_i} F(\xi_i')d\xi_i'd\xi_i \\ b &= k\int_0^1\int_0^{\xi_i} G(\xi_i')d\xi_i'd\xi_i \end{aligned}\right\}. \tag{14}$$

We have introduced the new baroclinicity parameters

$$\left.\begin{aligned} M_{x0} &= \frac{z_i}{u_*}\left(\frac{\partial U_g}{\partial z}\right)_0 \\ M_{y0} &= \frac{z_i}{u_*}\left(\frac{\partial V_g}{\partial z}\right)_0 \end{aligned}\right\}, \tag{15}$$

or, alternatively, $M_0 = (M_{x0}^2 + M_{y0}^2)^{\frac{1}{2}}$ and $\beta_0 = \tan^{-1}(M_{y0}/M_{x0})$, which are more appropriate than S_{x0} and S_{y0} because their use effectively eliminates the dependence of A_1' and B_1' on the parameter fz_i/u_*. Note that for the case of constant thermal wind, M_0 simply represents the difference in the magnitudes of geostrophic winds at the surface and at the top of the boundary layer normalized by u_*. It also has the advantage of not having f in the denominator and, hence, remaining well-behaved even near the equator.

Eqs. (8) and (13) are the main results of our simple model. General similarity considerations can only tell that A_{i0} and B_{i0} are some universal similarity functions of a host of parameters, *viz.* z_i/L, fz_i/u_*, M_{x0}, M_{y0}, and some parameters related to the variation of geostrophic shear with height. Separating out the effect of each empirically from rather difficult to make observations in the atmospheric boundary layer, in which all these parameters vary simultaneously (with the added complexities due to acceleration effects) seems to be an almost impossible task. Such efforts invariably end up in a large scatter of data from which only the strong trends are discernible (see, e.g., Arya, 1975; Clarke and Hess, 1974; Melgarejo and Deardorff, 1974). Here, by using simple arguments about the structure of the convective boundary layer, we have been able to separate A_{i0} or B_{i0} into a part (A_i or B_i) that is only dependent on z_i/L and fz_i/u_*, and another part (A_i' or B_i') that is dependent only on baroclinicity (M_0 and β_0), and have also predicted their approximate functional shapes.

The coefficients a and b depend on the variation of geostrophic shear with height. For the particular case of constant geostrophic shear ($F=G=1$), Eqs. (14) give $a=b=k/2$, while a value of $a=b=k/3$ is obtained for the case of linearly decreasing geostrophic shear ($F=G=1-\xi_i$). Thus deviations A_i' and B_i' due to baroclinicity should be 50% larger in the former case; under typical baroclinic conditions, these would be of the order of A_i and B_i.

According to this model the flow in the baroclinic mixed layer is far from geostrophic. Geostrophic balance is achieved in the inversion above, where U changes from its mixed-layer value $\langle U_g\rangle$ to the local U_g value, while V goes from essentially zero to the local V_g. Therefore we expect, in general, significant wind shear above the mixed layer. This leads to two effects which we have not considered in our simple model.

The first is that entrainment effects at the top of the mixed layer are likely to make H, the level where stress vanishes and geostrophic flow is achieved, larger than our rough estimate of z_i (Deardorff, 1974; Wyngaard and Coté, 1974). The second effect is due to the inertial oscillations in U and V about their equilibrium values U_g and V_g in the flow above the mixed layer. Some influence of these oscillations will be transmitted to the mixed layer by the entrainment process and will distort somewhat our flat, mixed layer velocity profiles.

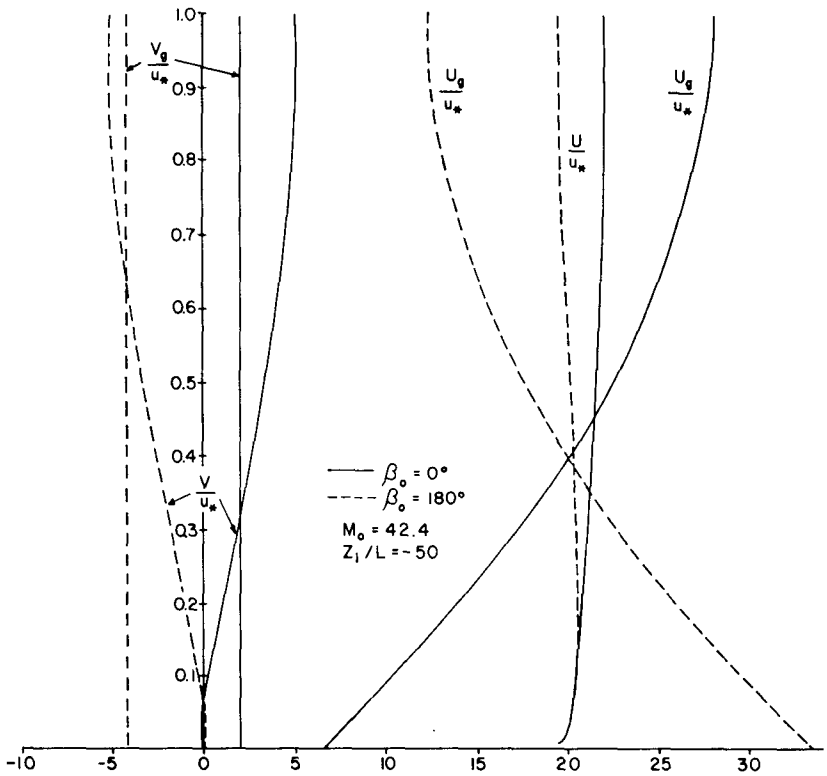

FIG. 1. The computed geostrophic and actual wind profiles in the mixed layer for $z_i/L = -50$ and $\beta_0 = 0°$ and 180°.

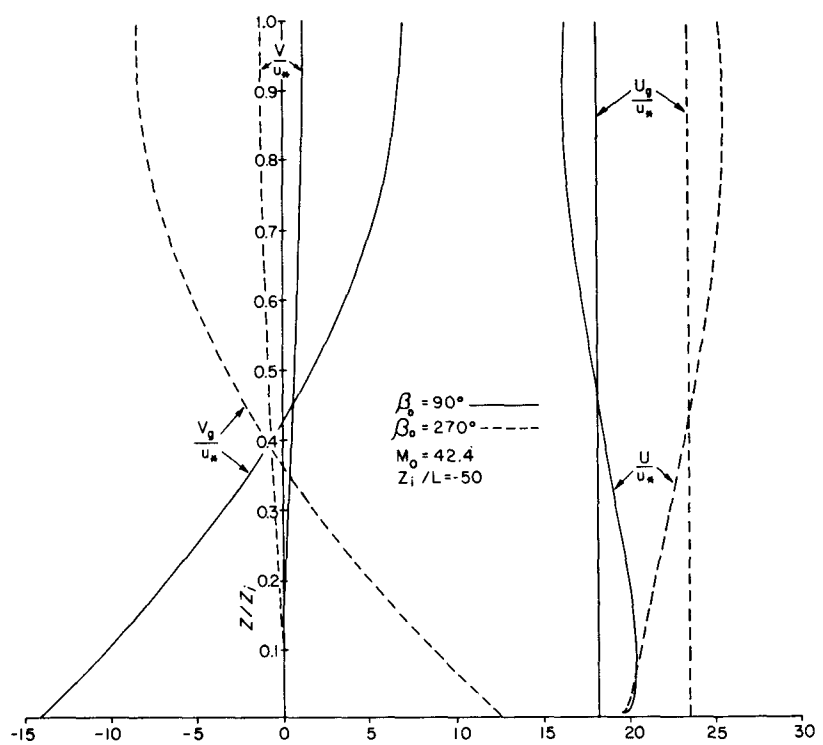

FIG. 2. As in Fig. 1 except for $\beta_0 = 90°$ and 270°.

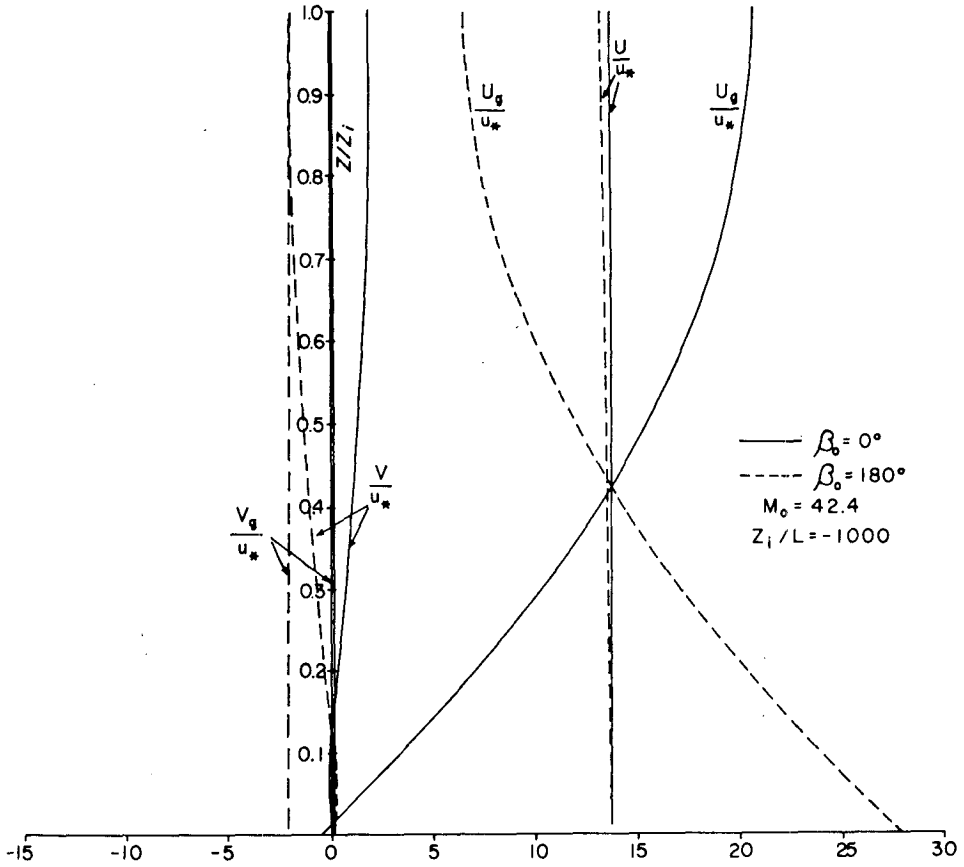

FIG. 3. The computed geostrophic and actual wind profiles in the mixed layer for $z_i/L=-1000$ and $\beta_0=0°$ and 180°.

This effect should not be large if the mixed layer turbulence time scale is small compared with that of the oscillation. This requires $z_i/w_* \ll f^{-1}$, where w_* $=(gQ_0z_i/T)^{\frac{1}{3}}$ is a characteristic mixed layer velocity scale. This can be rewritten as

$$\frac{u_*}{fz_i}\left(-\frac{z_i}{L}\right)^{\frac{1}{3}} \gg 1, \tag{16}$$

which is often satisfied in mid-afternoon convective situations.

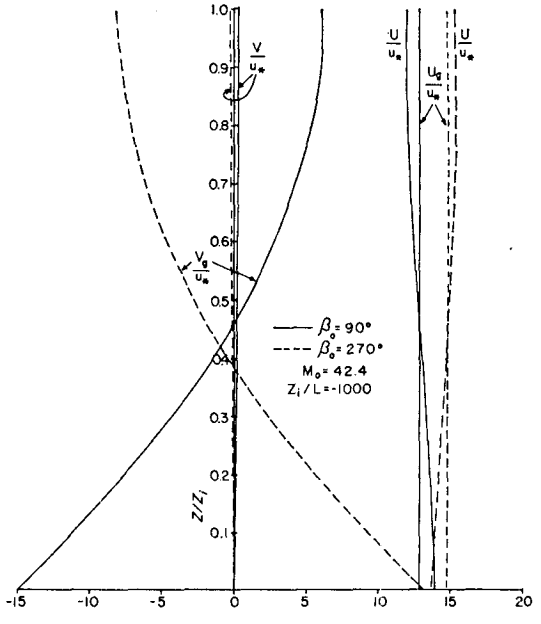

FIG. 4. As in Fig. 3 except for $\beta_0=90°$ and 270°.

4. Comparison with the results of higher-order closure model and observations

In order to check these deductions we use the higher-order closure model developed by Wyngaard *et al.* (1974b). This model is based on 14 coupled partial differential equations of mean gradients, variances, fluxes, and the turbulent energy dissipation. For the sake of simplicity, the inversion at the top is modeled as a rigid lid, although one can also allow for the entrainment from the stable layer above as in the case of a rising inversion (see Wyngaard and Coté, 1974). The model was run for several different magnitudes and orientations of geostrophic shear, which is assumed to be linearly decreasing with height and vanishing just below the inversion base ($F=G=1-\xi_i$), and for $z_i/z_0=3\times10^5$, $fz_i/u_*=0.133$ and 1, and $z_i/L=-50$ and -1000. We took west winds and the latitude $\phi=45°$N.

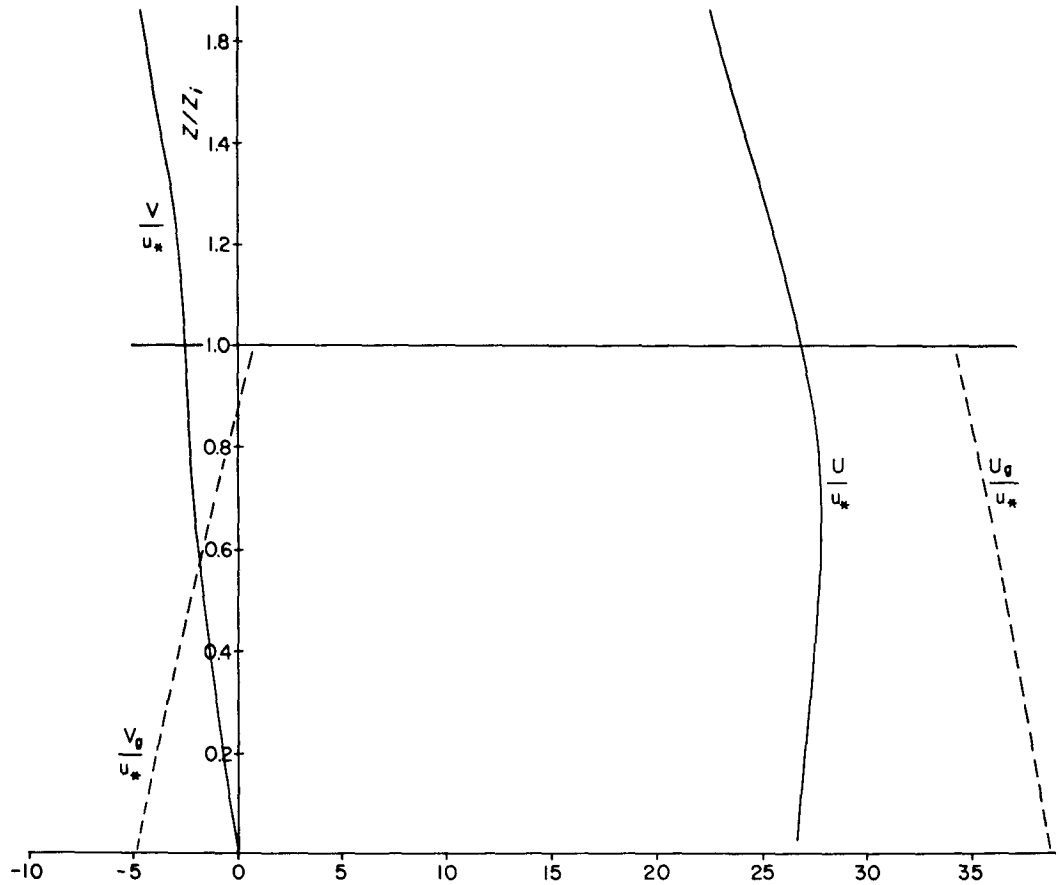

FIG. 5. The observed geostrophic and actual wind profiles from the Atlantic Trade Wind Experiment.

For the less convective case ($z_i/L=-50$), the computed wind and geostrophic wind profiles are presented in Fig. 1 for geostrophic shears oriented in the same or opposite direction to that of the surface wind. Fig. 2 represents the same for the cases of geostrophic shear normal to the surface wind direction, i.e., for cold or warm air advection. The values of the baroclinicity parameters M_0 and β_0 have been indicated on these figures. Note that the actual wind shears are small compared to the magnitude of the geostrophic shear ($M_0=42.4$ may be considered as an extreme case). In sign, $\partial U/\partial z$ in the bulk of the mixed layer follows $-\partial V_g/\partial z$, and $\partial V/\partial z$ follows $\partial U_g/\partial z$, just as argued in the previous section. The actual wind shears become negligibly small, however, with increasing instability, as seen from Figs. 3 and 4 for $z_i/L=-1000$. This implies that at least in the unstable boundary layer capped by an inversion, one cannot hope to determine geostrophic shear simply from the measured wind profile in the upper part of the boundary layer. Such a procedure has been incorrectly used by Venkatesh and Csanady (1974). Actually, the deviations from geostrophic equilibrium are most striking just below the inversion base; the return to equilibrium occurs in the stable layer above. Because of this, stress profiles develop strong curvature which may lead to greater stress magnitudes aloft than at the surface (see e.g., Wyngaard *et al.*, 1974a; Wyngaard and Coté, 1974).

Some observational evidence in support of our model results comes from a recent study by Brummer *et al.* (1974). Fig. 5 represents the 14-day averages of their observations over the ocean during the Atlantic Trade Wind Experiment (ATEX). During this period, the surface wind direction remained very steady and the surface geostrophic winds and geostrophic shears fairly steady, so that long-time averages (for eliminating the effects of accelerations) are meaningful. The mean value of $z_i\approx 600$ m is based on the average potential temperature profile; it is also about the average height of the subcloud layer. Fig. 5 shows that in the mixed layer wind shear magnitudes are much smaller than the magnitude of geostrophic shear. Large deviations from geostrophic equilibrium right up to the inversion base may be due to large momentum transport by cloud mixing (see Pennell and LeMone, 1974), some advective accelerations at these low latitudes, and possibly large errors in the determination of geostrophic winds from the only three shipborne pressure sensors. The above features of the mean wind profiles in the subcloud layer of the trades are also clearly evident in the

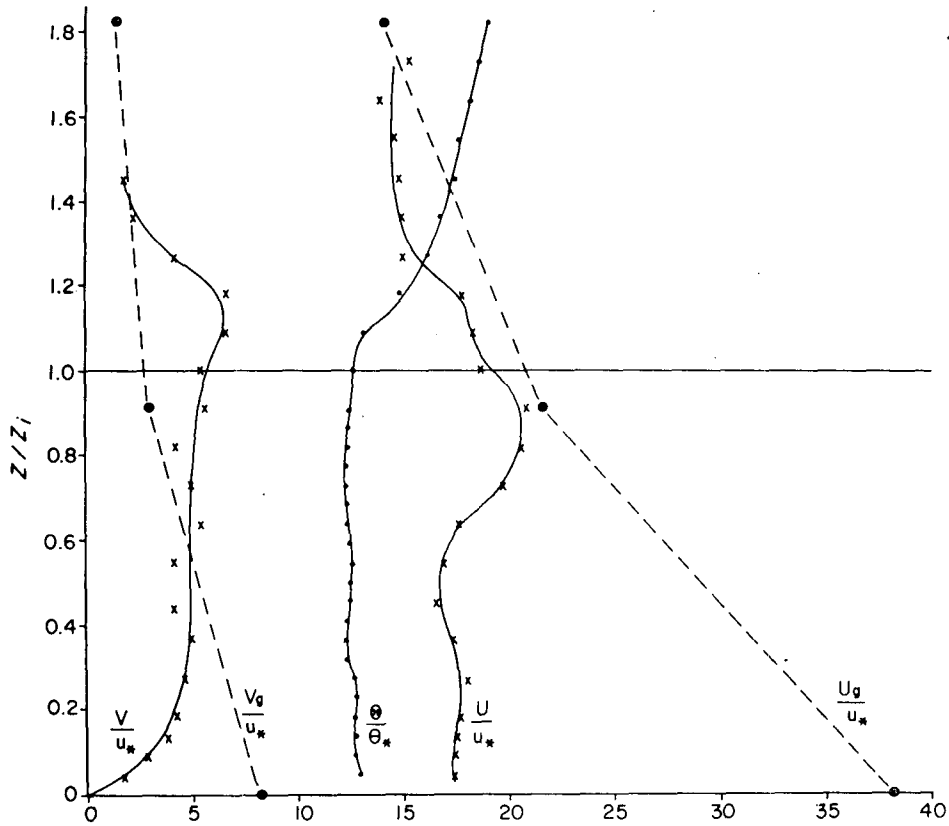

FIG. 6. The observed geostrophic and actual wind profiles on day 33 of the Wangara experiment.

Anegada observations gathered and reported by Charnock *et al.* (1956). Recent aircraft observations by Pennell and LeMone (1974) also indicate weak shears in the bulk of the mixed layer but strong shears just above the inversion base.

More experimental evidence is presented in Figs. 6 and 7 based on some daytime observations during the Wangara experiment (Clarke *et al.*, 1971). Here, the wind profiles are more irregular because of the smaller averaging period (each profile represents the average of 25 balloon soundings from five stations at 1100, 1200, 1300, 1400 and 1500 hours local time); some probably also show the effect of inertial oscillations or gravity waves arising from the entrainment process near the inversion (see, e.g. Deardorff, 1974; Wyngaard and Coté, 1974). The geostrophic wind profiles in Fig. 6 for day 33 are based on the observations from the radiosonde network; the geostrophic shears in the lower layer for this day are comparable to those derived from the surface temperature measurements from a smaller scale network of 13 stations. The profiles in Fig. 7 for other selected days (we particularly selected those for which z_i between 1200 and 1500 hours remained more or less constant) represent only the wind magnitudes. They all indicate insignificant shears in the bulk of the mixed layer even though the surface geostrophic shears or shears in the inversion layer were large. Here, M_0 and β_0 are based on the surface temperature data (see Clarke and Hess, 1974).

The computed results for the baroclinic (Figs. 3 and 4) and barotropic (not shown here) cases indicate that for the same z_i/z_0, z_i/L and fz_i/u_*, the layer-averaged values of actual and geostrophic winds are about the same, irrespective of baroclinicity. This verifies our basic assumption used in the derivation of the simple drag relations (7) and, hence, Eqs. (8) and (13) for the baroclinic convective boundary layer. A direct comparison of these with the results of the higher-order closure model is made in Figs. 8 and 9 for the case of linearly decreasing geostrophic shear ($a=b\approx 0.117$). Considering the crudeness of our simpler model on which Eqs. (13) are based, the agreement with the results of the more sophisticated numerical model is quite good, especially for the case of higher instability ($z_i/L=-1000$). Unlike (13), the numerical results indicate that A_i' and B_i' also depend very weakly on the parameters z_i/L and fz_i/u_*. These are more closely described by the slightly phase-shifted cosine and sine functions, i.e.,

$$\left.\begin{aligned} A_i' &= aM_0\cos(\beta_0-\delta) \\ B_i' &= bM_0\sin(\beta_0-\delta) \end{aligned}\right\}, \tag{17}$$

in which, according to our results, $\delta\approx 0°$ to 15°, the

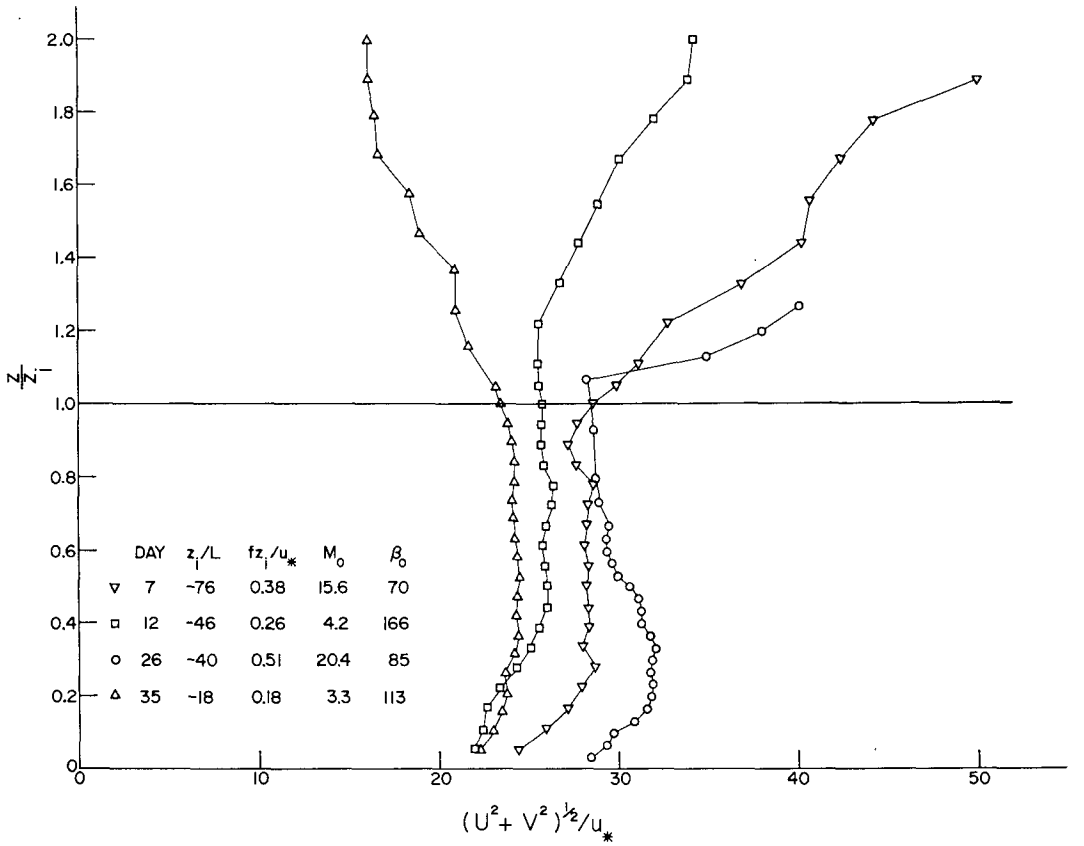

FIG. 7. Other examples of typical daytime wind profiles from the Wangara experiment.

actual value depending upon z_i/L and fz_i/u_*. Thus, $\partial A_{i0}/\partial M_{y0}$ and $\partial B_{i0}/\partial M_{x0}$ may not be exactly zero as indicated by (13), but could have magnitudes up to one-fourth that of $\partial A_{i0}/\partial M_{x0}=\partial B_{i0}/\partial M_{y0}\approx 0.11$. In sign, $\partial A_{i0}/\partial M_{y0}$ is expected to be positive and $\partial B_{i0}/\partial M_{x0}$ negative.

The above results can be compared with those from a recent study by Clarke and Hess (1974) based on the analysis of their Wangara data (Clarke *et al.*, 1971). Although their similarity functions A and B are somewhat different from A_{i0} and B_{i0} used here, their dependence on baroclinicity is expected to be similar. Their average results for all the unstable runs, when converted to our definitions of the baroclinicity parameters (taking an average value of $fz_i/u_*\approx 0.3$), give $\partial A/\partial M_{x0}\approx 0.08$, $\partial A/\partial M_{y0}\approx -0.04$, $\partial B/\partial M_{x0}\approx -0.11$ and $\partial B/\partial M_{y0}\approx 0.11$. The agreement with our computed results can be considered fair in view of the large uncertainties in the measurements of geostrophic shears and in the evaluation of A and B from experimental data.

Some observational evidence on the effect of geostrophic shear on the surface cross-isobaric angle is presented in Fig. 10. Here α_0', representing the deviation in α_0 from its barotropic value, is shown to be an oscillating function of β_0. The experimental curves represent the averages of the results obtained by Bernstein (1973) and Hoxit (1974) for their different sets of data; these have been converted to our definitions of thermal wind parameters (M_0,β_0) by assuming

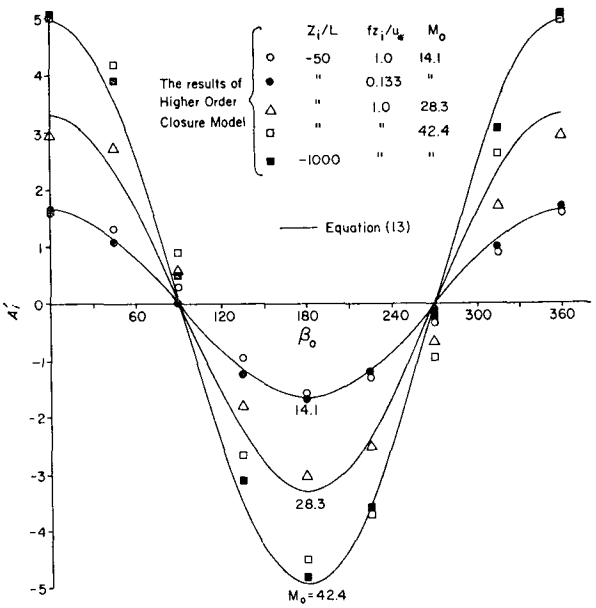

FIG. 8. Comparison of A_i' from Eq. (13) with the results of the higher-order closure model.

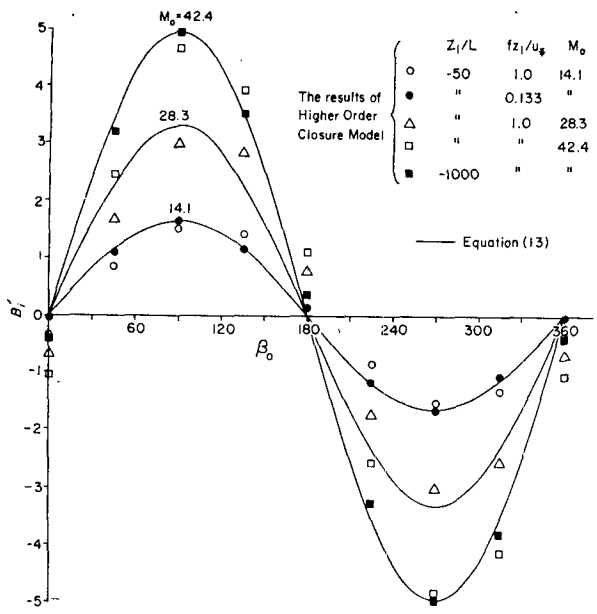

FIG. 9. Comparison of B_i' from Eq. (13) with the results of the higher-order closure model.

$u_*/G_0 \approx 0.03$. The average thermal stratification for these data is not known, but judging from the mean α_0 and the local times of soundings, it is expected to be near neutral or slightly stable. Therefore a comparison with our model results for the unstable boundary layer ($z_i/L = -50$) may not be strictly valid. There is still a good agreement in the positions of maximum and minimum in α_0' and theoretical amplitudes are comparable to those of the experimental curve due to Hoxit (1974). Bernstein's (1959, 1973) results indicating smaller amplitudes are considered to be less reliable because no corrections for geostrophic veering were made in determining α_0 from wind soundings.

Finally, we mention an interesting observation that the average value of α_0 over the oceans increases toward the equator, i.e., with decreasing $|f|$ (see, e.g., Riehl, 1954; Kraus, 1972; Brummer *et al.*, 1974). This trend is quite well explained by our simple drag relations (9) for the barotropic boundary layer recognizing that

$$\tan\alpha_0 = \frac{B_i(z_i/L,\ fz_i/u_*)}{\ln(z_i/z_0) - A_i\,(z_i/L, fz_i/u_*)} \approx \frac{u_*}{fz_i}\left[\ln\frac{z_i}{z_0} - A_i\right]^{-1} \quad (18)$$

In contrast to this, the drag laws proposed by Zilitinkevich *et al.* (1967), Clarke (1970) and Clarke and Hess (1974) give

$$\tan\alpha_0 = \frac{B(\mu)}{\ln(u_*/fz_0) - A(\mu)}, \quad (19)$$

in which $A(\mu)$ and $B(\mu)$ are some universal functions of only the stability parameter $\mu = ku_*/fL$. Note that Eq. (19) implies, in obvious conflict with observations, that α_0 should decrease toward the equator. This contradiction apparently arises from the assumption that the boundary layer height is proportional to u_*/f even in unstable conditions. Actually, as shown by Figs. 6 and 7, the boundary layer height is close to the height of the lowest inversion base, which is determined by many factors some of which considered external to the boundary layer dynamics (see e.g., Lilly, 1968; Stull, 1973; Deardorff, 1974).

A plot of z_i vs $u_*/|f|$ is given in Fig. 11, based on some observations from the Great Plains (Lettau and Davidson, 1957) and Wangara (Clarke *et al.*, 1971) experiments. Here the data points for each day are joined together by lines and are given a number identification which represents the day number for the Wangara data, and month and date for the Great Plains data. Obviously, there is no simple and unique relationship between the actual boundary layer height as determined by z_i and $u_*/|f|$ in unstable conditions. Such a relationship has been implied in the traditional similarity theory in which fH/u_* is considered a universal function of the stability parameter

$$\mu = \frac{ku_*}{|f|L} \sim \frac{g}{\bar{\theta}}\frac{\theta_*}{|f|u_*},$$

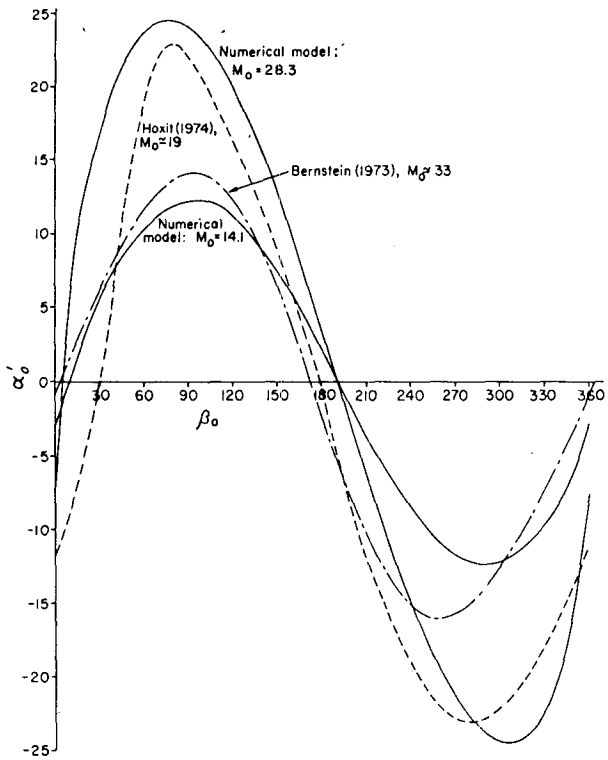

FIG. 10. Comparison of the observed deviations in the surface cross-isobar angle due to baroclinicity with the results of the higher-order closure model.

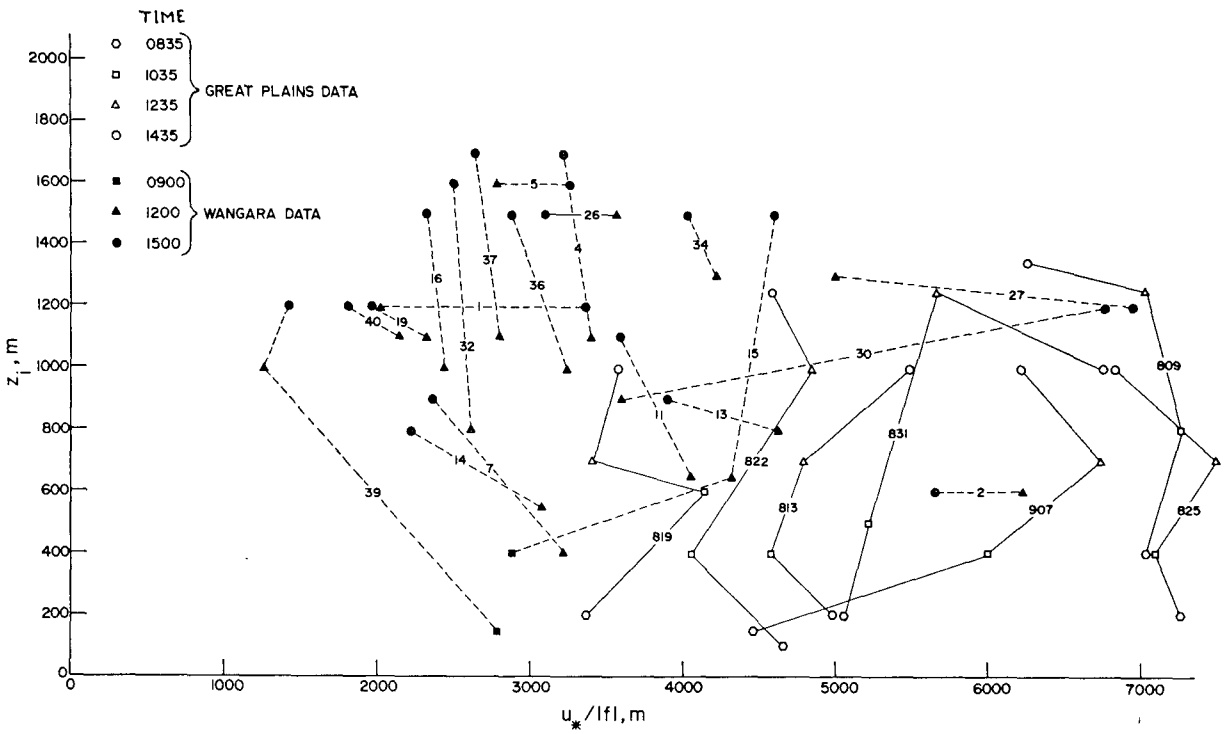

FIG. 11. Comparison of the observed boundary layer height z_i with $u_*/|f|$ based on some Great Plains and Wangara data.

where θ_* is the surface layer temperature scale and $g/\bar{\theta}$ the buoyancy parameter. Note that even if H and $u_*|f|$ are completely independent, a plot of fH/u_* against μ may show a spurious positive correlation between these two parameters mainly because of the common factor u_* in both and also because H and θ_* have qualitatively similar diurnal trends.

5. Conclusions

The baroclinicity effects in the atmospheric boundary layer, like stratification effects, are always present, but their influences on the structure and the parametric relations of the boundary layer have not received much attention. The K-theory models are not valid because they cannot consider the possible modifications of eddy viscosity or mixing length due to baroclinicity; the eddy viscosity concept itself becomes meaningless under convective conditions, which we have investigated here.

Based on the similarity and matching of inner and outer layer wind profiles, the surface geostrophic drag relations can be written in terms of some undetermined universal functions (Hess, 1973). For an unstable boundary layer capped by inversion, these similarity functions A_{i0} and B_{i0} must depend on at least four independent parameters. Separating out the effect of each empirically from observations under variable conditions in the atmosphere seems to be a very difficult task. We have been able to do this theoretically, however, by using a simple physical model of the convective boundary layer. Accordingly, each similarity function can be written as a sum of two parts, one depending only on z_i/L and fz_i/u_*, and the other depending only on the baroclinicity parameters M_0 and β_0. Our simple model also leads to the approximate but explicit forms of these functions.

The above drag laws and the basic model assumptions are supported by the results of the higher-order closure model developed by Wyngaard *et al.* (1974b) and also by observations in the atmosphere. In particular, they show that the actual wind shear magnitudes in the bulk of the mixed layer are small compared to the magnitude of geostrophic shear, and the deviations from geostrophic equilibrium are most striking just below the inversion base. Any approach to geostrophic equilibrium must occur in the stable layer above, which was not modeled here. The baroclinicity-dependent parts of A_{i0} and B_{i0} are shown to be approximately cosine and sine functions of the angle β_0 between the surface geostrophic shear and the surface wind, their amplitudes being proportional to M_0, the magnitude of the geostrophic shear normalized by z_i/u_*.

The surface cross-isobaric angle α_0 is also found to be an oscillating function of β_0 with larger values occurring under warm air advection and smaller values under cold air advection. The maximum and minimum values of α_0 are predicted to correspond to $\beta_0 \approx 90°$ and 290°, respectively, which are in fair agreement with the results of observations analyzed by Bernstein (1973)

and Hoxit (1974). Our drag relations also predict an increasing trend of α_0 toward the equator, which is also confirmed by observations. Quite the opposite trend is predicted by the geostrophic drag laws proposed by Zilitinkevich *et al.* (1967), Clark and Hess (1974), and others, who have assumed the boundary layer height to be proportional to u_*/f and have dropped z_i, the height of the lowest inversion base, altogether from similarity considerations.

Acknowledgments. We would like to thank Prof. J. A. Businger for a critical review of the manuscript and Mrs. Jo Ann Jarrett for typing the same. Partial support of the National Science Foundation under Grant GA-40648 is also acknowledged.

REFERENCES

Arya, S. P. S., 1975: Geostrophic drag and heat transfer relations for the atmospheric boundary layer. *Quart. J. Roy. Meteor. Soc.*, **101** (in press).

Bernstein, A. B., 1959: The effect of a horizontal temperature gradient on the surface wind. Unpublished M.S. thesis, Pennsylvania State University, 112 pp.

——, 1973: Some observations of the influence of geostrophic shear on the cross-isobar angle of the surface wind. *Boundary-Layer Meteor.*, **3**, 381–384.

Brummer, B., E. Augstein and H. Riehl, 1974: On the low-level wind structure in the Atlantic trade. *Quart. J. Roy. Meteor. Soc.*, **100**, 109–121.

Charnock, H., J. R. D. Francis and P. A. Sheppard, 1956: An investigation of wind structure in the trades. *Phil. Trans. Roy. Soc. London*, **A249**, 179–234.

Clarke, R. H., 1970: Observational studies in the atmospheric boundary layer. *Quart. J. Roy. Meteor. Soc.*, **96**, 91–114.

——, A. J. Dyer, R. R. Brock, D. G. Reid and A. J. Troup, 1971: The Wangara experiment: Boundary layer data. Tech. Paper No. 19, CSIRO, Div. Meteor. Phys., Australia, 362 pp.

——, and G. D. Hess, 1974: Geostrophic departure and the functions A and B of Rossby-number similarity theory. *Boundary-Layer Meteor.* (in press).

Deardorff, J. W., 1966: The countergradient heat flux in the lower atmosphere and in the laboratory. *J. Atmos. Sci.*, **23**, 503–506.

——, 1972: Numerical investigation of neutral and unstable planetary boundary layers. *J. Atmos. Sci.*, **29**, 91–115.

——, 1974: Three-dimensional numerical study of the height and mean structure of a heated planetary boundary layer. *Boundary-Layer Meteor.* **7**, 81–106.

Ellison, T. H., 1956: Atmospheric turbulence. *Surveys in Mechanics*, Cambridge University Press, 400–430.

Gray, W. M., and B. R. Mendenhall, 1973: A statistical analysis of factors influencing the wind veering in the planetary boundary layer. *Climatological Research*, The Hermann Flohn 60th Anniversary Volume, Meteor. Inst., University of Bonn, 167–194.

Hess, G. D., 1973: On Rossby-number similarity theory for a baroclinic planetary boundary layer. *J. Atmos. Sci.*, **30**, 1722–1723.

Hoxit, L. R.. 1974: Planetary boundary layer winds in baroclinic conditions. *J. Atmos. Sci.*, **31**, 1003–1020.

Kraus, E. B., 1972: *Atmospheric-Ocean Interaction.* Oxford University Press, 225 pp.

Lettau, H., 1967: Small to large-scale features of boundary layer structure over mountain slopes. *Proc. Symp. Mountain Meteorology*, E. R. Reiter and J. L. Rasmussen, Eds., 1–74.

——, and B. Davidson, 1957: *Exploring the Atmosphere's First Mile*, Vols. 1 and 2. Pergamon Press.

Lilly, D. K., 1968: Models of cloud-topped mixed layers under a strong inversion. *Quart. J. Roy. Meteor. Soc.*, **94**, 292–309.

Mahrt, L. J., and W. Schwerdtfeger, 1970: Ekman spirals for exponential thermal wind. *Boundary-Layer Meteor.*, **1**, 137–145.

Melgarejo, J. W., and J. W. Deardorff, 1974: Stability functions for the boundary-layer resistance laws based upon observed boundary-layer heights. *J. Atmos. Sci.*, **31**, 1324–1333.

Pennell, W. T., and M. A. LeMone, 1974: An experimental study of turbulence structure in the fair weather trade wind boundary layer. *J. Atmos. Sci.*, **31**, 1308–1323.

Riehl, H., 1954: *Tropical Meteorology.* McGraw-Hill, 392 pp.

Sheppard, P. A., H. Charnock and J. R. D. Francis, 1952: Observations of the westerlies over the sea. *Quart. J. Roy. Meteor. Soc.*, **78**, 563–582.

——, and H. H. Omar, 1952: The wind stress over the ocean from observations in the trades. *Quart. J. Roy. Meteor. Soc.*, **78**, 583–589.

Stull, R. B., 1973: Inversion rise model based on penetrative convection. *J. Atmos. Sci.*, **30**, 1092–1099.

Venkatesh, S., and G. T. Csanady, 1974: A baroclinic planetary boundary-layer model, and its applications to the Wangara data. *Boundary-Layer Meteor.*, **5**, 459–473.

Vorob'yev, V. I., 1969: The influence of nonstationarity and baroclinicity on the turbulence pattern in the atmospheric boundary layer. *Izv. Atmos. Ocean Phys.*, **5**, 56–69.

Wippermann, F., 1972: Baroclinic effects on the resistance law for the planetary boundary layer of the atmosphere. *Beitr. Phys. Atmos.*, **45**, 244–259.

Wyngaard, J. C., and O. R. Coté, 1974: The evolution of a convective planetary boundary layer: A higher-order-closure model study. *Boundary Layer Meteor.*, **7**, 289–308.

——, S. P. S. Arya and O. R. Coté, 1974a: Some aspects of the structure of convective planetary boundary layers. *J. Atmos. Sci.*, **31**, 747–754.

——, O. R. Coté and K. S. Rao, 1974b: Modeling the atmospheric boundary layer. *Advances in Geophysics*, Vol. 18A, Academic Press, 193–211.

Yordanov, D., and F. Wippermann, 1972: The parameterization of the turbulent fluxes of momentum, heat and moisture at the ground in a baroclinic planetary boundary layer. *Beitr. Phys. Atmos.*, **45**, 58–65.

Zilitinkevich, S. S., D. L. Laikhtman and A. S. Monin, 1967: Dynamics of the atmospheric boundary layer. *Izv. Atmos. Ocean Phys.*, **3**, 170–191.

——, and D. V. Chalikov, 1968: The laws of resistance and of heat and moisture exchange in the interaction between the atmosphere and an underlying surface. *Izv. Atmos. Ocean. Phys.*, **4**, 438–441.